6660–6675 Nucleic Acids Research, 2016, Vol. 44, No. 14 Published online 22 February 2016
doi: 10.1093/nar/gkw115

The MazF-regulon: a toolbox for the post-transcriptional stress response in *Escherichia coli*

Martina Sauert[1], Michael T. Wolfinger[2,3,4], Oliver Vesper[1], Christian Müller[1], Konstantin Byrgazov[1] and Isabella Moll[1,*]

[1]Max F. Perutz Laboratories, Center for Molecular Biology, Department of Microbiology, Immunobiology and Genetics, University of Vienna, Vienna Biocenter (VBC), Dr. Bohr-Gasse 9/4, A-1030 Vienna, Austria, [2]Max F. Perutz Laboratories, Department of Biochemistry and Molecular Cell Biology, University of Vienna, Vienna Biocenter (VBC), Dr. Bohr-Gasse 9/5, A-1030 Vienna, Austria, [3]Max F. Perutz Laboratories, Center for Integrative Bioinformatics Vienna, University of Vienna, Medical University of Vienna, Vienna Biocenter (VBC), Dr. Bohr-Gasse 9, A-1030 Vienna, Austria and [4]Institute for Theoretical Chemistry, University of Vienna, Währingerstraße 17, A-1090 Vienna, Austria

Received July 28, 2015; Revised February 16, 2016; Accepted February 17, 2016

ABSTRACT

Flexible adaptation to environmental stress is vital for bacteria. An energy-efficient post-transcriptional stress response mechanism in *Escherichia coli* is governed by the toxin MazF. After stress-induced activation the endoribonuclease MazF processes a distinct subset of transcripts as well as the 16S ribosomal RNA in the context of mature ribosomes. As these 'stress-ribosomes' are specific for the MazF-processed mRNAs, the translational program is changed. To identify this 'MazF-regulon' we employed Poly-seq (polysome fractionation coupled with RNA-seq analysis) and analyzed alterations introduced into the transcriptome and translatome after *mazF* overexpression. Unexpectedly, our results reveal that the corresponding protein products are involved in all cellular processes and do not particularly contribute to the general stress response. Moreover, our findings suggest that translational reprogramming serves as a fast-track reaction to harsh stress and highlight the so far underestimated significance of selective translation as a global regulatory mechanism in gene expression. Considering the reported implication of toxin-antitoxin (TA) systems in persistence, our results indicate that MazF acts as a prime effector during harsh stress that potentially introduces translational heterogeneity within a bacterial population thereby stimulating persister cell formation.

INTRODUCTION

During their lifetime, free-living bacteria have to deal with sudden environmental changes, e.g. in temperature, pH and nutrient availability, or to cope with the immune response and antibiotic treatment when invading a host. A general means to overcome adverse stress conditions is the stringent response, a bacterial survival mechanism by which the metabolism is reduced to a minimum. During the stringent response the alarmone guanosine tetra- or pentaphosphate (p)ppGpp is synthesized to trigger substantial alterations of the transcriptional program (1) by favoring alternative sigma factors that guide the RNA polymerase to the respective promoters (2). In addition, a variety of specific transcription factors can change the transcriptional landscape to ensure the physiological adaptation to the given conditions (3). Besides the transcriptional regulation, an increasing number of studies suggest that regulation at the post-transcriptional and translational level is likewise crucial for the modulation of protein synthesis, underlined by the rather imperfect correlation between tran-

*To whom correspondence should be addressed. Tel: +43 4277 54606; Fax: +43 1 4277 9546; Email: Isabella.moll@univie.ac.at
Present addresses:
Michael T. Wolfinger, Center for Anatomy and Cell Biology, MedicalUniversity of Vienna, Währingerstraße 13, 1090 Vienna, Austria.
Oliver Vesper, Center for Structural Systems Biology (CSSB),University Medical Center Eppendorf-Hamburg (UKE), Martinistrasse 52, D-20246 Hamburg, Germany, and Deutsches Elektronen-Synchrotron (DESY), Notkestrasse 85, D-22607 Hamburg, Germany.
Oliver Vesper, Institute of Molecular Biotechnology GmbH (IMBA), Austrian Academy of Sciences, Dr Bohr-Gasse 3-5, A-1030 Vienna, Austria.
Oliver Vesper, Research Institute of Molecular Pathology (IMP), Dr Bohr Gasse 7, A-1030 Vienna, Austria.
Konstantin Byrgazov, St. Anna Kinderkrebsforschung e.V., Department of Microbiology, Zimmermannplatz 10, A-1090 Vienna, Austria.

scriptomes and translatomes (4). Hitherto, known mechanisms for translational regulation involve e.g. regulatory small RNAs (sRNAs), riboswitches and regulatory proteins that can mask or expose ribosome binding sites or affect the RNA stability. However, in contrast to the global regulatory effect governed by alternative transcription these post-transcriptional mechanisms are rather specific for individual targets.

In striking contrast, we recently identified a post-transcriptional regulatory mechanism in *Escherichia coli* that has the potential to globally affect protein synthesis in response to a variety of different stress conditions (5). When cells encounter stress the toxin-antitoxin (TA) module *mazEF* is activated by proteolysis of the antitoxin MazE. Consequently, the free toxin MazF cleaves RNAs specifically at single-stranded ACA-sites leading to the rapid degradation of bulk mRNA and overall reduction of protein synthesis (6). Besides, MazF generates a subset of leaderless mRNAs (lmRNAs) by cleaving specific transcripts at ACA-sites upstream of the AUG start codon. Surprisingly, the 16S rRNA incorporated in mature ribosomes is likewise targeted by MazF. The endoribonuclease removes 43 nucleotides (nts) from the 16S rRNA 3′-end comprising the anti-Shine-Dalgarno (aSD) sequence (5). Thereby, $70S^{\Delta 43}$ ribosomes are generated that are incapable to initiate translation on canonical mRNAs containing a long and structured 5′-untranslated region (UTR) due to the lack of the SD/aSD interaction. However, the modified $70S^{\Delta 43}$ ribosomes were shown to selectively translate lmRNAs (5) constituting the so called stress translation machineries (STMs) (7).

Several studies addressing the physiological significance of chromosomally encoded TA systems, which are abundant in free-living bacteria but lost from strictly host-associated bacteria (8), suggest their implication in the general stress response and biofilm formation (9). Furthermore, the role of TA systems in growth arrest, (programmed) cell death and cell survival is widely discussed (10,11) and their influence on bacterial persistence, in particular during antibiotic treatment, has been shown (12–14). Persisters are supposed to be a metabolically inactive, dormant fraction of a bacterial population that is—despite being genetically identical to their non-persistent kin—tolerant to lethal concentrations of antibiotics (15). Thus, despite this transient nature of the tolerance phenotype, bacterial persistence poses a severe health problem during antibiotic treatment of pathogenic bacteria, which possess an usual high number TA loci (8,16). However, at present the underlying mechanisms are still poorly understood. Considering that MazF activity results in the processing of specific mRNAs as well as modification of the translational machinery, we hypothesized that this post-transcriptional stress response mechanism might contribute to the differentiation of some cells of a population into persister cells. Hitherto, only a few highly abundant proteins have been identified, that remain to be synthesized after *mazF* activation employing 2D gel electrophoresis and mass spectrometry (17). As Vesper *et al*. have shown that about 50% of the ribosomes are cleaved by MazF after serine hydroxamate (SHX) treatment mimicking amino acid starvation (5), it is conceivable that this mechanism targets many more transcripts. To determine the so-called 'MazF-regulon', i.e. the entity of processed and selectively translated mRNAs after *mazF* overexpression, we employed a Poly-seq analysis, combining polysome fractionation and next generation RNA sequencing. In contrast to the ribosome profiling analysis developed by Ingolia *et al*. (18), our approach is suitable to isolate intact, full length mRNAs from polysomes and thereby enables the concomitant analysis of the translatome and the processing state of the polysome-associated mRNA. Hence, our results provide insights into the linkage between transcription and translation levels and represent a snapshot of the altered transcriptional and translational landscape in dependence of MazF activity.

MATERIALS AND METHODS

Bacterial strains and growth conditions used in this study

Escherichia coli strain MC4100 F' (19) was used for the analysis in the absence of *mazF* overexpression. For the analysis upon *mazF* overexpression the same strain was transformed with plasmid pSA1 harboring the *lacI*^{q} gene as well as *mazF* under the control of the T5 promoter and the lac operator (17). Bacterial strains were grown at 37°C in Luria-Bertani (LB) broth, supplemented with 100 μg/ml ampicillin when required for plasmid maintenance. Growth was monitored by photometric measurement of the optical density at 600 nm.

Purification of total and polysome-associated RNA upon *mazF* overexpression

E. coli strains MC4100 F' and MC4100 F' pSA1 were grown at 37°C in LB. At OD_{600} of 0.5, strain MC4100 F' pSA1 was treated with 100 μM IPTG for 15 min and then harvested by centrifugation. MC4100 F' was harvested without treatment at an OD_{600} of 0.6. For total RNA preparation, 50 ml of cell cultures were harvested by centrifugation for 10 min at 4000 rpm and 4°C in an Eppendorf 5810 R centrifuge (Rotor FA 45–6–30) and cell pellets were frozen in liquid nitrogen. Total RNA was isolated using TRIzol®-reagent (Invitrogen) following the manufacturer's protocols.

For preparation of polysome-associated RNA 1.2 l of cell culture per sample were quickly chilled by pouring into 3x 500 ml centrifuge bottles (Nalgene) containing 100 g of fresh ice, while kept in an ice-water-bath (1:1 v/v) containing 10 g/l NaCl and immediately harvested by centrifugation at 4000 rpm for 10 min at 4°C in a Sorvall RC5-C (FiberLite F10S-6×500y rotor, Piramon Technologies). Cell pellets were kept on ice and gently resuspended in ice-cold TICO-lysis-buffer (TICO-buffer: 20 mM HEPES, 6 mM MgOAc, 6 mM NH_4OAc, 4 mM β-Mercapto-EtOH plus 4 mg/ml Lysozyme) to a final concentration of 200 OD_{600}-units per ml, transferred to a 50 ml conical centrifuge tube (Starlab), and slowly frozen at −20°C to avoid shearing of RNA. For gentle cell disruption the suspension was slowly thawed on ice and slowly refrozen at −20°C for three times. DNase I (RNase-free, Roche) was added in a concentration of 0.05 units per OD_{600}-unit and incubated for 10 min on ice after each thawing step. The S30 extracts were cleared in aliquots of 1 ml by centrifugation in 1.5 ml reac-

tions tubes (Sarstedt) at 30.000 g for 1 h at 4°C in a Sigma 3K30 centrifuge (rotor 12154) and stored at −80°C.

A total of 50–100 A_{260}-units of S30 extracts (in a maximum of 1 ml) were loaded onto a 10–30% sucrose gradient in TICO-buffer in SW28 tubes (SETON) to separate ribosomal subunits, monosomes and polysomes by centrifugation at 28.000 rpm for 3 h at 4°C in a Beckmann L-70 ultracentrifuge (Beckmann SW28 rotor). Upon fractionation, polysome fractions (Figure 1B, fractions 20–32, ∼13 ml) were pooled and concentrated to 300 μl in H_2O-DEPC by precipitation with 10% sodium acetate (pH 5,2) and 50% 2-propanol over night at −20°C followed by centrifugation at 13.000 rpm for 1 h at 4°C in a Eppendorf 5810 R centrifuge (Rotor FA 45–6–30). RNA was isolated using TRIzol®-reagent (Invitrogen) following the manufacturer's protocols.

To remove accidentally co-purified genomic DNA from total or polysome derived RNA, the samples were treated with DNase I (RNase-free, Roche), extracted again with phenol/chloroform and ethanol-precipitation. Complete removal of DNA was verified by PCR (Primers for chromosomal *grcA*: I3/G1, data not shown). Ribosomal RNA was depleted using Ribo-Zero™ Magnetic Kit (Gram-Negative Bacteria, Epicentre) following the manufacturer's protocol. For further analysis, the depleted rRNA, bound to the magnetic beads, was recovered by phenol/chloroform extraction and ethanol-precipitation. For an overview of the purification process and efficiencies see the Supplementary Table S1.

Library preparation and next-generation sequencing

For the comparative RNA-seq analysis the following samples were used: Total RNA from untreated MC4100 F' cells ('T-') and from MC4100 F' pSA1 cells 15 min after induction of *mazF* overexpression by IPTG ('T+'), and polysome-associated mRNA from untreated MC4100 F' cells ('P-') and from MC4100 F' pSA1 cells 15 min after induction of *mazF* overexpression by IPTG ('P+'). Libraries from two biological replicates (R1 and R2) were prepared using 50–100 ng of the rRNA-depleted RNA using NEBNext® Ultra Directional RNA Library Prep Kit for Illumina (New England BioLabs), following the manufacturer's protocol. The quality of the resulting adaptor ligated cDNA was checked with the Agilent DNA Kit on an Agilent 2100 Bioanalyzer. Library preparation resulted in samples with average fragment sizes of 200–240 bp (data not shown). Samples were pooled (one set of four ('T-', 'T+', 'P-', 'P+') per replicate for one multiplex) and sequenced on Illumina HiSeq2000 with a single read length of 100 bp (VBCF NGS Unit; www.vbcf.ac.at). Sequence reads were mapped to the *E. coli* BW2952 MC4100 reference sequence (accession NC_012759).

Computational analysis

The sequencing resulted in a total of ∼220 million raw reads per multiplex/replicate. Sequencing adapters were removed from the de-multiplexed samples with *cutadapt* (20). Quality control before and after adapter removal was performed with *FastQC* (http://www.bioinformatics.babraham.ac.uk/projects/fastqc). The BW2952 MC4100 reference genome and annotations (accession NC_012759) were obtained from the NCBI FTP server and reads were mapped against the reference genome with *segemehl* (v0.1.7) (21,22). Uniquely mapped reads were extracted for the downstream analysis and processed for UCSC visualization. Read count numbers for each sample were determined with the *htseq-count* utility from the *HTSeq* package (23) and differential gene expression analysis was performed with *DESeq* (24). Cutoff values for considering changes as significant are padj < 0.05 and log2fold change < -0.6 for down-regulation and > 0.6 for up-regulation. Visualization of aligned reads and coverage profiles were done with the UCSC genome browser (25). Coverage profiles of individual samples were normalized (26).

To cluster candidates according to their functions we used the function assignments provided by *EcoGene 3.0* (27). We downloaded a table of gene names, protein products and functions for all 4506 annotated genes (status of December 2014) and used the provided information to cluster the genes into the following functional classes: Metabolism and energy supply (ME), Cell cycle (CC), Protein synthesis (PS), Response regulation (RR), Cell structure (CS), Not classified (NC). See Supplementary Table S3 for a detailed list of the defined functional classes and subclasses. The matching of lists of candidates with the classification annotation list was performed with the R statistics software (28).

RESULTS

Purification of total and polysome-associated mRNA

In light of the hypothesized role of the *mazEF* module in cell survival and persister cell formation, our observation that MazF activity leads to reprogramming of protein synthesis prompted us to simultaneously analyze alterations introduced by MazF in the *E. coli* transcriptome and translatome. As an initial approach we ectopically overexpressed *mazF* in *E. coli* strain MC4100 F' harboring plasmid pSA1 (17). The cells were grown in LB medium until mid-exponential phase, and 15 min after induction of *mazF* overexpression by addition of IPTG, total RNA ('T+') was isolated from two biological replicates for transcriptome analysis. Likewise, total RNA was prepared from untreated MC4100 F' cells ('T-'). Concomitantly, we prepared S30 extracts, which were separated on sucrose density gradients to subsequently isolate mRNAs from the polysome fractions ('P-' and 'P+') as schematically depicted in Figure 1A. In contrast to sequencing analysis of total RNA after *mazF* overexpression, which reveals the processing state of all RNAs in general, this additional step allows the determination of the entity of mRNAs that are selectively translated by the $70S^{\Delta 43}$ ribosomes and therefore associated to polysomes.

Polysomes are assemblies of 70S ribosomes translating simultaneously the same mRNA molecule (29), thus mRNAs associated to polysomes represent the translatome. In contrast to the state of the art method for polysome-based translatome analysis described by Ingolia *et al.* (18), we isolated full length mRNAs from polysomes without the use of translational inhibitors, to avoid a bias on the

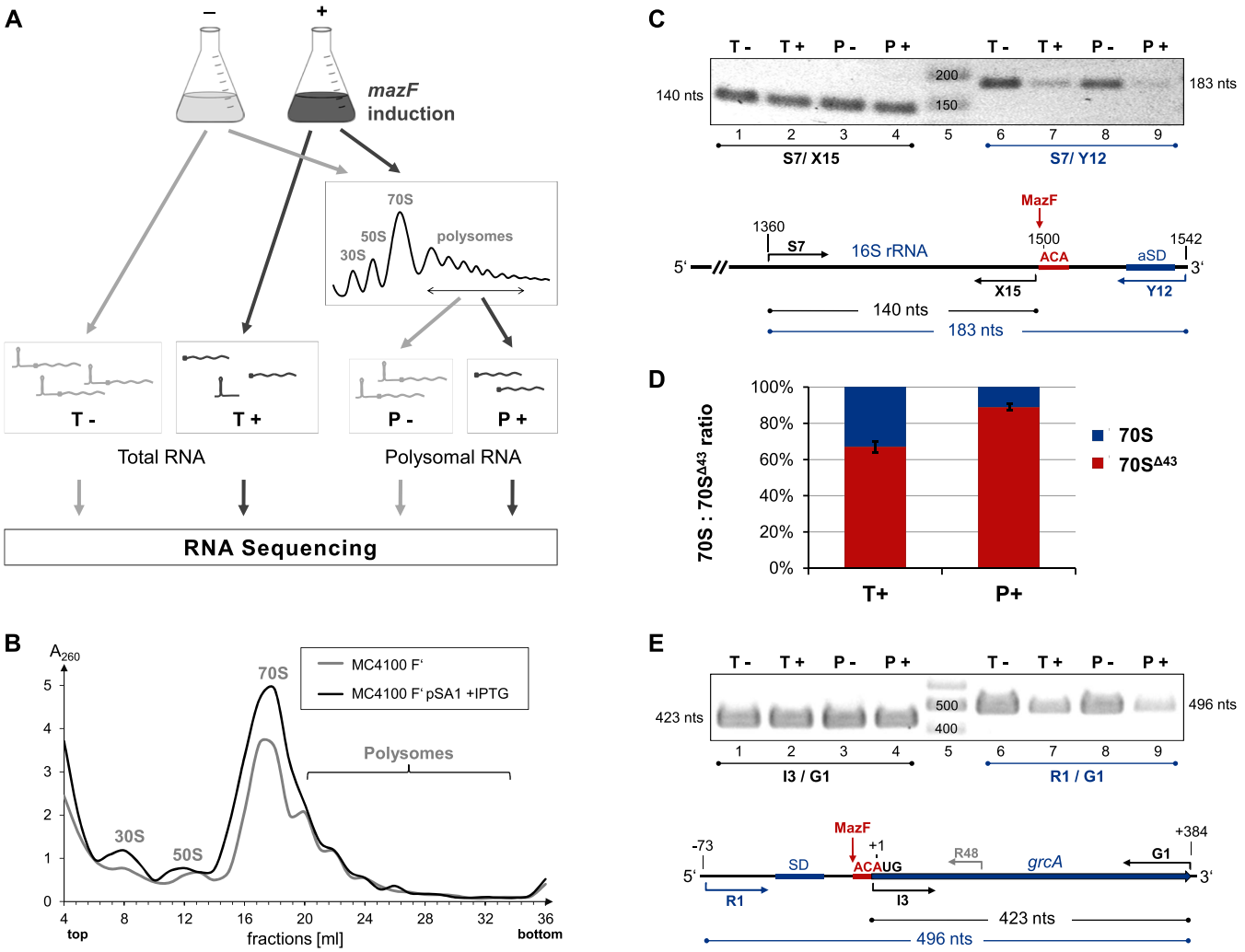

Figure 1. The RNA purification and validation of the method. (**A**) Schematic depiction of the workflow. *E. coli* MC4100 F' (light gray, '-') and MC4100 F' pSA1 (dark gray, '+') were cultured and *mazF* overexpression was induced in MC4100 F' pSA1 by addition of IPTG at OD_{600} of 0.5. Fifteen minutes thereafter total RNA was extracted ('T') and S30 extracts were subjected to sucrose density gradient centrifugation to obtain ribosome profiles shown in (**B**). RNA was isolated from the pooled polysome fractions ('P'). All samples of two independent experiments were subjected to RNA-seq. (**C**) Processing of the 16S rRNA was determined by RT-PCR analysis performed on rRNA from total and polysomal RNA using forward primer S7 and reverse primers X15 or Y12 that bind upstream or downstream of the MazF-cleavage site, respectively, as indicated below. Lanes 1–4: RT-PCR with S7 and X15 served as internal control. Lanes 6–9: RT-PCR with S7 and Y12. (**D**) Signals obtained in the RT-PCR analysis shown in (C) were quantified and normalized. The 70S:$70S^{\Delta 43}$ ratios calculated for the total ('T+') and polysomal ('P+') RNA purified after *mazF* overexpression are given. (**E**) RT-PCR on *grcA* mRNA in total and polysomal RNA using forward primers R1 or I3 that bind upstream or downstream of the MazF-cleavage site, respectively, as indicated below, and reverse primer G1. Lanes 1–4: RT-PCRs with I3 and G1 served as internal control. Lanes 6–9: RT-PCR with R1 and G1.

stress response. Furthermore, we disrupted the cells gently using lysozyme and three freeze-and-thaw cycles to avoid shearing of the RNA and degradation of the non-immobilized polysomes. The ribosomal subunits, monosomes and polysomes were separated by sucrose density gradient centrifugation of cell lysates. As shown in Figure 1B, the overall inhibition of translation after *mazF* induction is indicated by less pronounced polysome peaks (black line) when compared to ribosome profiles obtained from exponentially growing cells (gray line). The polysome fractions (Figure 1B, fractions 20–34) were pooled omitting the monosome peak in order to select for actively translated mRNAs. The respective RNA was isolated and upon depletion of rRNA *via* magnetic beads (Ribozero®, Epicenter; see Supplementary Table S1, rows 'P-' and 'P+', column 'rRNA depletion') subjected to RNA-seq (see Materials and Methods).

Validation of rRNA and mRNA processing by MazF

First, we confirmed the formation of the $70S^{\Delta 43}$ ribosomes upon *mazF* overexpression. To this end, the rRNA recovered from magnetic beads used for depletion of the above mentioned RNA samples was subjected to reverse transcription PCR (RT-PCR). To distinguish between full length 16S rRNA (nts 1–1542) and MazF-processed $16S^{\Delta 43}$ rRNA (nts 1–1499), two different reverse primers specific for the 16S rRNA sequence upstream (X15) or downstream (Y12) of the MazF cleavage site were used in combination

with the forward primer S7, which anneals to a central region of the 16S rRNA (Figure 1C). Employing primer pair S7/X15, which anneals to both, intact and truncated 16S rRNA, we obtained comparable amounts of the expected product in all samples tested, without treatment (lanes 1 and 3) and upon overexpression of *mazF* (lanes 2 and 4), revealing that the same amount of rRNA was used in all RT-PCR analyses. Using primer pair S7/Y12, which is specific for the full length 16S rRNA, we obtained significantly weaker signals when using rRNA purified from cells upon *mazF* overexpression (lane 7 and 9) when compared to the sample taken from untreated cells (lane 6 and 8). Remarkably, quantification and normalization of the data indicated that 15 min after *mazF* induction more than 65% of the ribosomes are processed. Intriguingly, about 90% of the ribosomes present in the polysome fractions are $70S^{\Delta 43}$ ribosomes (Figure 1D). Together, these results not only prove the formation of $70S^{\Delta 43}$ ribosomes by MazF in general, they further underline that translationally active ribosomes after *mazF* overexpression are predominantly $70S^{\Delta 43}$ ribosomes, which lack the 3′-terminal 43 nts of the 16S rRNA due to MazF cleavage.

Next, the quality of isolated total and polysome-associated mRNA was assessed *via* RT-PCR using the *grcA* mRNA that has been previously identified as MazF target (formerly *yfiD*) (5). The encoded protein GrcA represents the glycine radical co-factor A that reactivates pyruvate formate lyase after oxidative stress (30). Active MazF cleaves at an ACA-site at position -2 relative to the A of the AUG start codon resulting in the selective translation of the leaderless *grcA* mRNA by the $70S^{\Delta 43}$ ribosomes. We confirmed the MazF-processing by primer extension (Supplementary Figure S2A) and RT-PCR analysis using polysomal RNA (Figure 1E). To discriminate between full length *grcA* mRNA comprising the 5′-UTR and the leaderless *grcA* mRNA variant we performed RT-PCR with reverse primer G1, hybridizing within the *grcA* coding region, in combination with either I3, annealing at the 5′-end of the *grcA* coding region downstream of the MazF cleavage site, or R1, binding to the 5′-UTR upstream of the MazF cleavage site (Figure 1E). RT-PCR performed with primers I3/G1 specific for both full length and leaderless *grcA* yielded the same amounts of the 423 nts long PCR product in all four samples tested (Figure 1E, lanes 1–4). In contrast the amount of the PCR products using primers R1/G1 specific for the full length *grcA* mRNA was significantly reduced in RNA extracted from cells after *mazF* overexpression (lanes 7). Using mRNA purified from polysomes the amount of this product is even further reduced (Figure 1E, lane 9) indicating that the actively translated *grcA* mRNA upon MazF activation is predominantly leaderless.

Taken together, these data reveal that the employed polysome purification procedure is appropriate to extract sufficient amounts of intact mRNA for downstream applications like RNA-sequencing. Thus, the polysome-associated mRNAs as well as the total RNAs were used to generate cDNA libraries that were subjected to deep sequencing as described in Material and Methods to identify transcripts that are selectively translated upon *mazF* overexpression thereby constituting the 'MazF-regulon'.

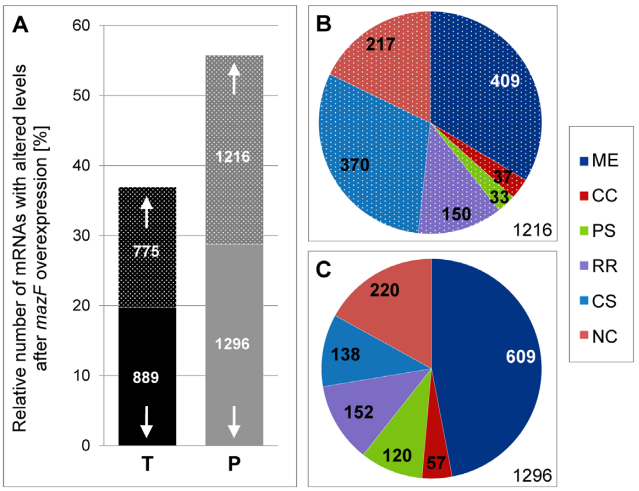

Figure 2. Alteration of mRNA levels after *mazF* overexpression in total and polysome-associated mRNAs. (**A**) The ratio between mRNAs with significantly increased (dotted) and decreased (plain) levels in total RNA (black) and polysome-associated mRNA (gray) after *mazF* overexpression is shown relative to the total number of *E. coli* genes, according to *EcoGene3.0* (27). Absolute numbers are indicated in each bar. (**B**) Distribution of polysome-associated mRNAs with significantly increased levels into the different functional clusters. (**C**) Distribution of polysome-associated mRNAs with significantly decreased levels into the different functional clusters. The absolute numbers of RNAs assigned to each functional cluster are indicated and represent the numbers given in Supplementary Table S2, columns 'P up A' and 'P down A'. (ME = metabolism and energy supply, CC = cell cycle, PS = protein synthesis, RR = response regulation, CS = cell structure, NC = not classified).

Selective translation plays a crucial regulatory role after *mazF* overexpression

First, we characterized MazF-mediated changes introduced in the transcriptome and translatome employing a differential gene expression (DGE) analysis with *DESeq* (24) on the read count data obtained from total and polysome-associated RNA-seq data mapped with the short read aligner *segemehl* (21,22). We only considered transcripts with an adjusted *P*-value (padj) < 0.05 and a log2fold change > 0.65 or < -0.65 (3-fold change) significantly differentially abundant between the two conditions ($\pm$*mazF* overexpression). We found that upon *mazF* overexpression the levels of 1664 transcripts are significantly changed in total RNA, amongst those are 889 down-regulated and 775 up-regulated (Figure 2A). These numbers indicate that MazF induces a plethora of changes within only 15 min, as this number corresponds to 37% of the genome. This effect is even more pronounced in the polysome-associated mRNA fraction, where the levels of 2511 transcripts, representing 56% of the genome, are significantly altered (Figure 2A). Upon *mazF* overexpression 1296 mRNAs are less abundant in polysomes, whereas 1216 transcripts are more abundant. Additionally, we observed, that the transcript level alterations in total RNA and polysome-associated RNA do not entirely overlap (Supplementary Figure S1A and B).

Given these substantial alterations in total and polysome-associated mRNA levels, we next determined the physiological functions of the proteins encoded by the affected mR-

NAs applying a functional cluster analysis based on information provided by *EcoGene 3.0* (27) as specified in detail in Materials and Methods (also see Supplementary Table S3). We observed that almost half of the mRNAs, whose translation is reduced after *mazF* overexpression are functionally involved in the general cell 'metabolism and energy supply' (Figure 2C, dark blue). This result goes in line with the observations that activation of the toxin MazF leads to down-regulation of cellular metabolism (14). Our analysis further revealed that the levels of a rather large fraction of mRNAs that classify into 'protein synthesis' are decreased in polysomes after *mazF* overexpression and that correspondingly only the levels of 33 transcripts of this functional cluster are increased (Figure 2B and C, respectively, light green). Taken together, these results suggest that the 'protein synthesis' cluster is an example for negative regulation on the basis of selective protein synthesis during stress (also shown in Supplementary Figure S1C). By contrast, a large fraction of mRNAs that show augmented levels in polysomes after *mazF* overexpression, is involved in 'cell structure' (Figure 2B, light blue and Supplementary Figure S1C) indicating their selective translation after the stress.

Notably, the cluster specific MazF-induced transcript level alterations are only apparent when analyzing polysome-associated mRNA (Supplementary Table S2 and Supplementary Figure S1C). Likewise, the difference in mRNA abundance between total and polysome-associated mRNA is more pronounced after *mazF* overexpression (see Supplementary Figure S1D). Taken together, these observations strongly support the notion that the translational adaption by the means of specialized ribosomes plays a significant role in the MazF-triggered stress response and suggest that MazF induces a first-level, fast-track stress response by generating the $70S^{\Delta 43}$ ribosomes.

The 'MazF-regulon'

Finally, we analyzed the processing state of selectively translated mRNAs present in the polysomes after *mazF* overexpression. To this end, we screened the read count density profiles visualized in the UCSC genome browser (25) for variations in the transcript coverage (Table 1). In contrast to the expected generation of lmRNAs, this analysis revealed that MazF processing not only occurs directly upstream of the AUG start codon as shown for the *grcA* mRNA (Figure 1E and Supplementary Figure S2A), but also can take place up to 100 nts upstream of the start codon yielding a processed but still leadered mRNA harboring a SD sequence. Nonetheless, these MazF-processed but leadered mRNAs are still predominantly associated to polysomes, i.e. they are actively translated. To validate the MazF-mediated processing at the observed ACA-sites in the 5′-UTR of 15 selected mRNAs with cleavage sites between one to 25 nts upstream of the start codon we performed primer extension analysis on total RNA (Figure 3 and Supplementary Figure S2). Further, we confirmed that in correspondence to the sequencing data the *erfK* and *infA* mRNAs despite comprising ACA-sites in their 5′-UTR are not cleaved by MazF at these positions (data not shown).

Further analysis of the MazF-regulon, comprising the 330 processed and significantly polysome-associated mRNAs (listed in Table 1) revealed no particular functional clustering of the corresponding protein products (Figure 4A). We observed that transcripts with functions in 'metabolism and energy supply' and 'protein synthesis' are slightly overrepresented compared to the distribution of functional clusters among all *E. coli* genes (Figure 4B), whereas 'not classified' RNAs and RNAs with function in 'cell structure' are slightly underrepresented. This shows that the MazF-mediated stress response has a more wide-ranging impact then expected. Interestingly, 52 of the 330 (16%) processed mRNA, constituting the MazF-regulon, are essential. As only 7% of the *E. coli* genes are essential, this high number supports our hypothesis that the MazF-regulon represents a subset of mRNAs, essential or important for the bacterial population to survive during and to recover after stress.

Selective translation of MazF-processed mRNAs

The unexpected observation that the MazF-regulon not only comprises lmRNAs but also processed transcripts with 5′-UTRs that still harbor a SD sequence is difficult to reconcile with the selective translation by $70S^{\Delta 43}$ ribosomes that lack the aSD sequence. Thus, we tested for translation initiation complex formation by $70S^{\Delta 43}$ ribosomes employing the full length and the MazF processed variants of the *rpsU* and the *groL* mRNAs as examples for a lmRNA generated by MazF cleavage directly upstream of the AUG start codon (5) and a MazF-processed mRNA that still harbors a 5′-UTR comprising the SD-sequence generated by cleavage 25 nts upstream of the start codon, respectively (Figure 5). As shown in Figure 5A, toeprinting analysis employing the canonical *rpsU* mRNA comprising the 47 nts long 5′-UTR revealed that in contrast to 30S subunits (lane 2) isolated $70S^{\Delta 43}$ ribosomes do not form translation initiation complexes (lane 3). However, on the leaderless *rpsU* transcript the $70S^{\Delta 43}$ ribosomes are proficient to selectively form initiation complexes at the 5′-terminal AUG start codon (lane 4) whereas only a very weak toeprinting signal was detectable when canonical 30S subunits were used (lane 5). These results are in line with the selective translation of lmRNAs by $70S^{\Delta 43}$ ribosomes described by Vesper *et al*. (5). Using the two *groL* mRNA variants comprising either the canonical 5′-UTR of 152 nts or only 25 nts after MazF-processing, respectively (Figure 5B and C), the analysis revealed that $70S^{\Delta 43}$ ribosomes are able to form a translation initiation complex on the MazF-processed transcript despite the presence of a 25 nts long 5′-UTR (Figure 5C, lane 8). As expected, we did not observe a toeprinting signal of the $70S^{\Delta 43}$ ribosomes when using the full length *groL* mRNA (lane 3). This result exemplifies that $70S^{\Delta 43}$ ribosomes are proficient to selectively translate MazF-processed transcripts even if they harbor a truncated 5′-UTR comprising the SD sequence.

DISCUSSION

The MazF-mediated stress response poses a novel prime example for a fast and energy-efficient post-transcriptional regulation mechanism in bacteria. Solely by triggering the degradation of one protein, namely the antitoxin MazE,

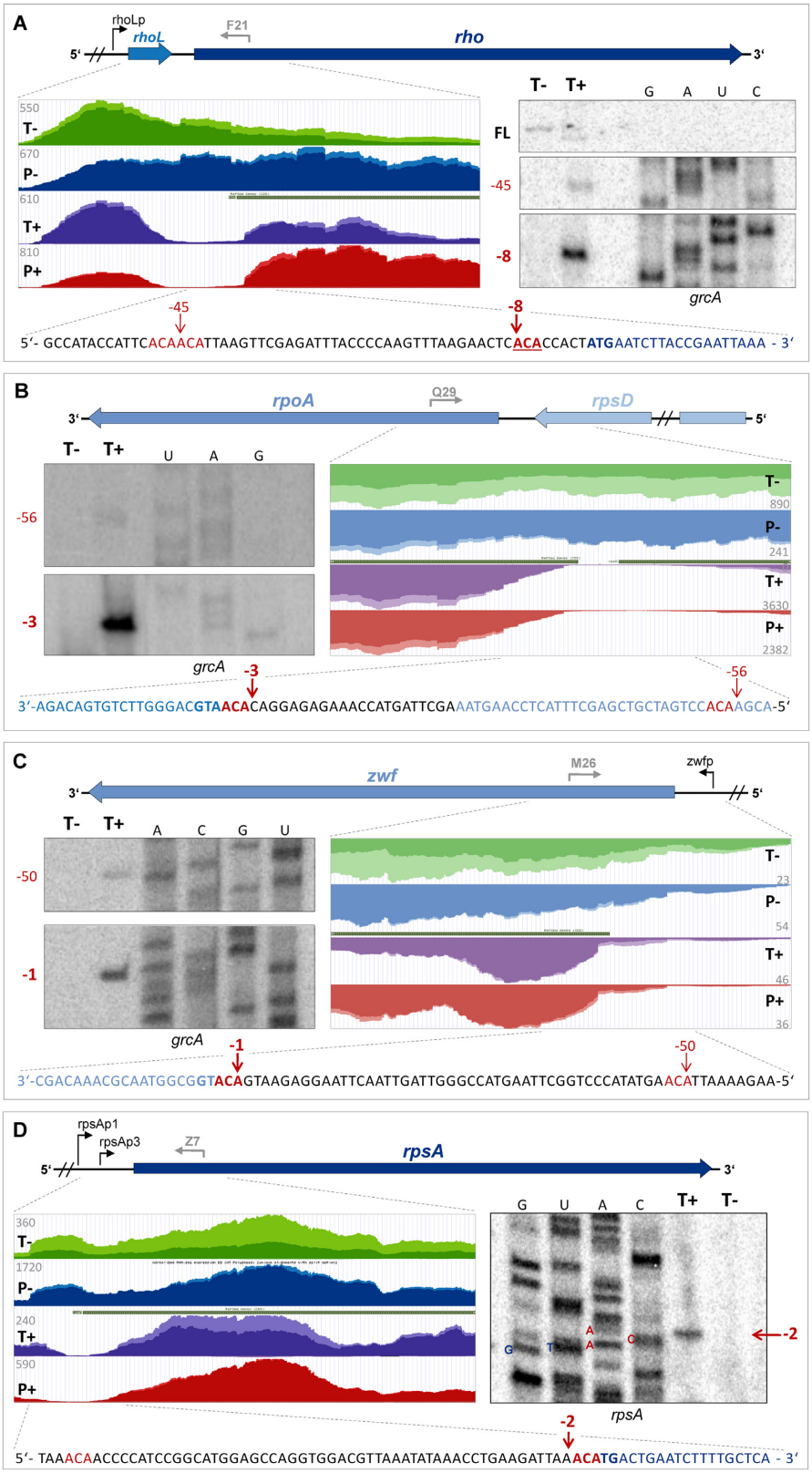

Figure 3. Validation of the MazF target mRNAs (**A**) *rho*, (**B**) *rpoA*, (**C**) *zwf* and (**D**) *rpsA*, respectively by primer extension analysis. Gene loci of the respective transcripts are schematically depicted by blue arrows. Positions of primers used for the analysis are indicated by gray arrows. The coverage profiles of sequencing reads performed on total RNA ('T', green and purple) and RNA extracted from polysomes ('P', blue and red) from *E. coli* cells during exponential growth ('-', green and blue) or 15 min after *mazF* overexpression ('+', purple and red) aligned to the respective genes and the corresponding primer extension analyses are shown. Sequencing reactions were performed using *in vitro* transcribed *grcA* (A, B and C) or *rpsA* mRNAs (D), respectively. Below the nucleotide sequences of the respective regions are given. The coding region is highlighted in blue, the AUG start codon is shown in bold and the MazF cleavage sites are highlighted in red.

Table 1. The MazF-regulon. All MazF-processed and significantly polysome-associated mRNAs identified by the Poly-seq analysis are listed

Gene	cleaved ACA [Distance to start in nts]	Protein product	Classification
mutH	2	methyl-directed mismatch repair protein	CC
mscL	2	mechanosensitive channel protein, high conductance	CS
tatC	2	TatABCE protein translocation system subunit	CS
aroG	2	3-deoxy-D-arabino-heptulosonate-7-phosphate synthase, phenylalanine repressible	ME
cycA	2	D-alanine/D-serine/glycine transporter	ME
ptrB	2	protease II	ME
sppA	2	protease IV (signal peptide peptidase)	ME
yggG	2	Phe-Phe periplasmic metalloprotease, OM lipoprotein; low salt-inducible; Era-binding heat shock protein	ME
srlB	2	glucitol/sorbitol-specific enzyme IIA component of PTS	ME
pdxY	2	pyridoxamine kinase	ME
nadC	2	quinolinate phosphoribosyltransferase	ME
grcA	2	autonomous glycyl radical cofactor	ME
zwf	2	glucose-6-phosphate 1-dehydrogenase	ME
gatZ	2	D-tagatose 1,6-bisphosphate aldolase 2, subunit	ME
glpK	2	glycerol kinase	ME
mltD	2	predicted membrane-bound lytic murein transglycosylase D	ME
fabD	2	malonyl-CoA-[acyl-carrier-protein] transacylase	ME
ispD	2	4-diphosphocytidyl-2C-methyl-D-erythritol synthase	ME
amn	2	AMP nucleosidase	ME
nrdA	2	ribonucleoside-diphosphate reductase 1, alpha subunit	ME
nupG	2	nucleoside transporter	ME
proS	2	prolyl-tRNA synthetase	ME
yajG	2	putative lipoprotein	NC
ybgL	2	UPF0271 family protein	NC
yjeI	2	DUF4156 family lipoprotein	NC
rpmB	2	50S ribosomal subunit protein L28	PS
rpsA	2	30S ribosomal subunit protein S1	PS
rpsU	2	30S ribosomal subunit protein S21	PS
rsuA	2	16S rRNA pseudouridine(516) synthase	PS
rpoN	2	RNA polymerase, sigma 54 (sigma N) factor	PS
srmB	2	ATP-dependent RNA helicase	PS
engA	2	GTPase; multicopy suppressor of ftsJ	RR
ygiW	2	hydrogen peroxide and cadmium resistance periplasmic protein; stress-induced OB-fold protein	RR
uspD	2	stress-induced protein	RR
ftsA	3	ATP-binding cell division protein involved in recruitment of FtsK to Z ring	CC
ftsE	3	cell division ATP-binding protein	CC
mltA	3	membrane-bound lytic murein transglycosylase A	CS
btuB	3	vitamin B12/cobalamin outer membrane transporter	CS
yadS	3	UPF0126 family inner membrane protein	CS
exbB	3	membrane spanning protein in TonB-ExbB-ExbD complex	CS
ffh	3	Signal Recognition Particle (SRP) component with 4.5S RNA (ffs)	CS
ynaI	3	mechanosensitive channel protein, very small conductance	CS
ptsH	3	phosphohistidinoprotein-hexose phosphotransferase component of PTS system (Hpr)	ME
srlA	3	glucitol/sorbitol-specific enzyme IIC component of PTS	ME
visC	3	2-octaprenylphenol hydroxylase, FAD-dependent	ME
yqjH	3	putative siderophore interacting protein	ME
kdsC	3	3-deoxy-D-manno-octulosonate 8-phosphate phosphatase	ME
artI	3	arginine transporter subunit	ME
grxD	3	glutaredoxin-4	NC
yeaQ	3	UPF0410 family protein	NC
yoaH	3	UPF0181 family protein	NC
ytfK	3	DUF1107 family protein	NC
rplB	3	50S ribosomal subunit protein L2	PS
rpoA	3	RNA polymerase, alpha subunit	PS
trmJ	3	tRNA mC32,mU32 2′-O-methyltransferase, SAM-dependent	PS
cpxR	3	response regulator in two-component regulatory system with CpxA	RR
mdoG	4	OPG biosynthetic periplasmic beta-1,6 branching glycosyltransferase	CS
ydeE	4	putative transporter	CS
lgt	4	phosphatidylglycerol-prolipoprotein diacylglyceryl transferase	ME
glnP	4	glutamine transporter subunit	ME
wecH	4	O-acetyltransferase for enterobacterial common antigen (ECA)	ME
yqaE	4	cyaR sRNA-regulated protein	NC
greA	4	transcript cleavage factor	PS
tig	5	peptidyl-prolyl cis/trans isomerase (trigger factor)	CC
yhhQ	5	DUF165 family inner membrane protein	CS
ynaJ	5	DUF2534 family putative inner membrane protein	CS

Table 1. Continued

Gene	cleaved ACA [Distance to start in nts]	Protein product	Classification
ilvL	5	ilvG operon leader peptide	ME
radA	5	DNA repair protein	ME
uxuR	5	fructuronate-inducible hexuronate regulon transcriptional repressor; autorepressor	ME
yafV	5	putative NAD(P)-binding C-N hydrolase family amidase	ME
yfcF	5	glutathione S-transferase	ME
ppiD	5	periplasmic folding chaperone, has an inactive PPIase domain	NC
ydcJ	5	putative metalloenzyme	NC
yacL	5	UPF0231 family protein	NC
ytfJ	5	putative transcriptional regulator	NC
yceA	5	putative rhodanese-related sulfurtransferase	NC
yeaO	5	DUF488 family protein	NC
yhdV	5	putative outer membrane protein	NC
rplR	5	50S ribosomal subunit protein L18	PS
rtcB	5	RNA-splicing ligase	PS
rnd	5	ribonuclease D	PS
emrA	5	multidrug efflux system	RR
treR	5	trehalose 6-phosphate-inducible trehalose regulon transcriptional repressor	RR
yceN	6	putative lipid II flippase	CS
ynjC	6	putative ABC transporter permease	CS
thrL	6	thr operon leader peptide	ME
glgB	6	1,4-alpha-glucan branching enzyme	ME
caiC	6	putative crotonobetaine/carnitine-CoA ligase	ME
vacJ	6	ABC transporter maintaining OM lipid asymmetry, OM lipoprotein component	ME
apt	6	adenine phosphoribosyltransferase	ME
gsk	6	inosine/guanosine kinase	ME
nrdB	6	ribonucleoside-diphosphate reductase 1, beta subunit, ferritin-like protein	ME
ydfZ	6	selenoprotein, function unknown	NC
ygiB	6	DUF1190 family protein	NC
rlmB	6	23S rRNA mG2251 2′-O-ribose methyltransferase, SAM-dependent	PS
yddM	6	putative DNA-binding transcriptional regulator	RR
yjhU	6	putative DNA-binding transcriptional regulator; KpLE2 phage-like element	RR
katG	6	catalase-peroxidase HPI, heme b-containing	RR
ygaZ	7	putative L-valine exporter, norvaline resistance protein	ME
mukE	7	chromosome condensin MukBEF, MukE localization factor	NC
pgm	8	phosphoglucomutase	ME
uhpA	8	response regulator in two-component regulatory system wtih UhpB	ME
coaA	8	pantothenate kinase	ME
pflA	8	pyruvate formate-lyase 1-activating enzyme; [formate-C-acetyltransferase 1]-activating enzyme; PFL activase	ME
fadH	8	2,4-dienoyl-CoA reductase, NADH and FMN-linked	ME
htrG	8	SH3 domain protein	NC
rho	8	transcription termination factor	PS
ampH	9	D-alanyl-D-alanine-carboxypeptidase/endopeptidase; penicillin-binding protein; weak beta-lactamase	CS
yidC	9	membrane protein insertase	CS
hisQ	9	histidine ABC transporter permease	ME
glmM	9	phosphoglucosamine mutase	ME
ugpQ	9	glycerophosphodiester phosphodiesterase, cytosolic	ME
lrp	9	leucine-responsive global transcriptional regulator	ME
ycbZ	9	putative peptidase	NC
yeaT	9	transcriptional activator of dmlA	RR
murA	10	UDP-N-acetylglucosamine 1-carboxyvinyltransferase	CS
rplL	10	50S ribosomal subunit protein L7/L12	PS
sohA	10	antitoxin of the SohA(PrlF)-YhaV toxin-antitoxin system	RR
yhcM	11	divisome ATPase	CC
shiA	11	shikimate transporter	CS
rbsK	11	ribokinase	ME
yjcE	11	putative cation/proton antiporter	NC
zipA	12	FtsZ stabilizer	CC
ivbL	12	ilvB operon leader peptide	ME
ndk	12	multifunctional nucleoside diphosphate kinase and apyrimidinic endonuclease and 3′-phosphodiesterase	ME
yhiR	12	23S rRNA m(6)A2030 methyltransferase, SAM-dependent	PS
phoB	12	response regulator in two-component regulatory system with PhoR	RR
yjgJ	12	transcriptional repressor for divergent bdcA	RR
iadA	13	isoaspartyl dipeptidase	ME
metL	13	Bifunctional aspartokinase/homoserine dehydrogenase 2	ME
yhhK	13	PanD autocleavage accelerator, panothenate synthesis	ME
fpr	13	ferredoxin-NADP reductase; flavodoxin reductase	ME

Table 1. Continued

Gene	cleaved ACA [Distance to start in nts]	Protein product	Classification
gnd	13	6-phosphogluconate dehydrogenase, decarboxylating	ME
yjjG	13	dUMP phosphatase	ME
rpsP	13	30S ribosomal subunit protein S16	PS
ydeP	13	putative oxidoreductase	RR
hcaR	14	hca operon transcriptional regulator	ME
dipZ	14	thiol:disulfide interchange protein and activator of DsbC	ME
fdoG	14	formate dehydrogenase-O, large subunit	ME
rhsC	14	Rhs protein with putative toxin domain; putative neighboring cell growth inhibitor	RR
dnaQ	15	DNA polymerase III epsilon subunit	CC
fimE	15	tyrosine recombinase/inversion of on/off regulator of fimA	CS
fliY	15	cystine transporter subunit	CS
dcuA	15	C4-dicarboxylate antiporter	ME
murP	15	N-acetylmuramic acid permease, EIIBC component, PTS system	ME
yciO	15	putative RNA binding protein	NC
yadH	15	putative ABC transporter permease	NC
bdm	15	biofilm-dependent modulation protein	RR
yfiB	16	OM lipoprotein putative positive effector of YfiN activity	CS
ydcS	16	putative ABC transporter periplasmic binding protein	CS
btuE	16	glutathione peroxidase	ME
sixA	16	phosphohistidine phosphatase	ME
yjfJ	16	PspA/IM30 family protein	NC
yeiS	16	DUF2542 family protein	NC
yhcB	16	DUF1043 family inner membrane-anchored protein	NC
yjbR	16	DUF419 family protein	NC
rpsG	16	30S ribosomal subunit protein S7	PS
lepA	16	back-translocating elongation factor EF4, GTPase	PS
lexA	16	transcriptional repressor of SOS regulon	RR
yggE	16	oxidative stress defense protein	RR
yfjD	17	UPF0053 family inner membrane protein	CS
yjiY	17	putative transporter	CS
ptsI	17	PEP-protein phosphotransferase of PTS system (enzyme I)	ME
atpE	17	F0 sector of membrane-bound ATP synthase, subunit c	ME
yniA	17	fructosamine kinase family protein	NC
imp	17	LPS assembly OM complex LptDE, beta-barrel component	RR
seqA	18	negative modulator of initiation of replication	CC
frdA	18	anaerobic fumarate reductase catalytic and NAD/flavoprotein subunit	ME
fabI	18	enoyl-[acyl-carrier-protein] reductase, NADH-dependent	ME
nlpC	18	putative C40 clan peptidase lipoprotein	ME
rpsT	18	30S ribosomal subunit protein S20	PS
feaR	18	transcriptional activator for tynA and feaB	RR
dnaN	19	DNA polymerase III, beta subunit	CC
sstT	19	sodium:serine/threonine symporter	CS
nepI	19	putative transporter	CS
fbp	19	fructose-1,6-bisphosphatase I	ME
galU	19	glucose-1-phosphate uridylyltransferase	ME
gatB	19	galactitol-specific enzyme IIB component of PTS	ME
cysQ	19	3′(2′),5′-bisphosphate nucleotidase	ME
nuoM	19	NADH:ubiquinone oxidoreductase, membrane subunit M	ME
wbbK	19	lipopolysaccharide biosynthesis protein	ME
thyA	19	thymidylate synthetase	ME
pepB	19	aminopeptidase B	ME
infC	19	translation initiation factor IF-3	PS
efp	19	polyproline-specific translation elongation factor EF-P	PS
prfA	19	peptide chain release factor RF-1	PS
marA	19	multiple antibiotic resistance transcriptional regulator	RR
nagZ	19	beta N-acetyl-glucosaminidase	RR
yobA	19	CopC family protein	RR
mdtK	20	multidrug efflux system transporter	CS
ilvD	20	dihydroxyacid dehydratase	ME
mtlA	20	mannitol-specific PTS enzyme: IIA, IIB and IIC components	ME
gapA	20	glyceraldehyde-3-phosphate dehydrogenase A	ME
rsd	20	stationary phase protein, binds sigma 70 RNA polymerase subunit	RR
rfaB	21	lipopolysaccharide 1,6-galactosyltransferase; UDP-D-galactose:(glucosyl)lipopolysaccharide-1,6-D-galactosyltransferase	CS
aroH	21	3-deoxy-D-arabino-heptulosonate-7-phosphate synthase, tryptophan repressible	ME
kefG	22	potassium-efflux system ancillary protein for KefB, glutathione-regulated	CS
aroP	22	aromatic amino acid transporter	ME
clpX	22	ATPase and specificity subunit of ClpX-ClpP ATP-dependent serine protease	ME
araF	22	L-arabinose ABC transporter periplasmic binding protein	ME

Table 1. Continued

Gene	cleaved ACA [Distance to start in nts]	Protein product	Classification
accB	22	acetyl CoA carboxylase, BCCP subunit	ME
folE	22	GTP cyclohydrolase I	ME
fadD	22	acyl-CoA synthetase (long-chain-fatty-acid–CoA ligase)	ME
lepB	23	leader peptidase (signal peptidase I)	CS
glpF	23	glycerol facilitator	ME
garR	23	tartronate semialdehyde reductase	ME
metF	23	5,10-methylenetetrahydrofolate reductase	ME
yjcZ	23	YjcZ family protein; yhjH motility defect suppressor	NC
yebZ	23	inner membrane protein	RR
clcB	24	H(+)/Cl(-) exchange transporter	CS
pepP	24	proline aminopeptidase P II	ME
panC	24	pantothenate synthetase	ME
pdxJ	24	pyridoxine 5′-phosphate synthase	ME
acnB	24	aconitate hydratase 2; aconitase B; 2-methyl-cis-aconitate hydratase	ME
ynjH	24	DUF1496 family protein	NC
yfiH	24	UPF0124 family protein	NC
frr	24	ribosome recycling factor	PS
ygdD	25	UPF0382 family inner membrane protein	CS
pabC	25	4-amino-4-deoxychorismate lyase component of para-aminobenzoate synthase multienzyme complex	ME
napB	25	nitrate reductase, small, cytochrome C550 subunit, periplasmic	ME
aphA	25	acid phosphatase/phosphotransferase, class B, non-specific	ME
ytfB	25	OapA family protein	NC
rpmI	25	50S ribosomal subunit protein L35	PS
groL	25	Cpn60 chaperonin GroL, large subunit of GroSL	RR
sbcB	26	exodeoxyribonuclease I; exonuclease I	CC
bacA	26	undecaprenyl pyrophosphate phosphatase	RR
ygcJ	26	CRISP RNA (crRNA) containing Cascade antiviral complex protein	RR
ubiE	27	bifunctional 2-octaprenyl-6-methoxy-1,4-benzoquinone methylase/ S-adenosylmethionine:2-DMK methyltransferase	ME
yniC	27	2-deoxyglucose-6-P phosphatase	ME
yodD	27	uncharacterized protein	RR
cysU	28	sulfate/thiosulfate ABC transporter permease	CS
yidQ	28	DUF1375 family outer membrane protein	NC
yigZ	28	UPF0029 family protein	NC
yhaH	29	DUF805 family inner membrane protein,	CS
metQ	29	DL-methionine transporter subunit	ME
speA	29	biosynthetic arginine decarboxylase, PLP-binding	ME
nrfA	29	nitrite reductase, formate-dependent, cytochrome	ME
udk	29	uridine-cytidine kinase	ME
hfq	29	global sRNA chaperone; HF-I, host factor for RNA phage Q beta replication	RR
aer	29	fused signal transducer for aerotaxis sensory component/methyl accepting chemotaxis component	RR
yjbB	30	putative Na+/Pi-cotransporter	CS
dsbA	30	periplasmic protein disulfide isomerase I	PS
tnaB	31	tryptophan transporter of low affinity	ME
otsB	31	trehalose-6-phosphate phosphatase, biosynthetic	RR
pstS	32	phosphate ABC transporter periplasmic binding protein	CS
rimM	32	ribosome maturation factor	PS
otsA	32	trehalose-6-phosphate synthase	RR
argT	34	lysine/arginine/ornithine transporter subunit	ME
livJ	34	branched-chain amino acid ABC transporter periplasmic binding protein	ME
pepN	34	aminopeptidase N	ME
pagB	34	lipid A phosphoethanolamine transferase	ME
hokD	34	Qin prophage; small toxic polypeptide	RR
hflB	35	protease, ATP-dependent zinc-metallo	ME
narP	35	response regulator in two-component regulatory system with NarQ	ME
yejG	35	uncharacterized protein	NC
rimN	35	tRNA(ANN) t(6)A37 threonylcarbamoyladenosine modification protein, threonine-dependent ADP-forming ATPase	PS
ygaW	36	alanine exporter, alanine-inducible, stress-responsive	ME
hybC	36	hydrogenase 2, large subunit	ME
yciK	36	putative EmrKY-TolC system oxoacyl-(acyl carrier protein) reductase	ME
rpoD	36	RNA polymerase, sigma 70 (sigma D) factor	PS
cmoA	36	carboxy-SAM synthase	PS
hslO	36	heat shock protein Hsp33	RR
gatC	37	pseudogene, galactitol-specific enzyme IIC component of PTS	ME
plsC	37	1-acyl-sn-glycerol-3-phosphate acyltransferase	ME
gloA	38	glyoxalase I, Ni-dependent	ME

Table 1. Continued

Gene	cleaved ACA [Distance to start in nts]	Protein product	Classification
ygcK	38	CRISP RNA (crRNA) containing Cascade antiviral complex protein	RR
iscX	39	Fe(2+) donor and activity modulator for cysteine desulfurase	NC
cheZ	39	chemotaxis regulator, protein phosphatase for CheY	RR
yfbV	40	UPF0208 family inner membrane protein	CS
yaaJ	40	putative transporter	ME
dgkA	40	diacylglycerol kinase	ME
sbmA	41	peptide antibiotic transporter	RR
hslU	41	molecular chaperone and ATPase component of HslUV protease	RR
aroB	42	3-dehydroquinate synthase	ME
yqeF	42	short chain acyltransferase	ME
cysW	43	sulfate/thiosulfate ABC transporter permease	CS
dmsD	43	twin-argninine leader-binding protein for DmsA and TorA	ME
rlmL	43	23S rRNA m(2)G2445 and m(7)G2069 methyltransferases, SAM-dependent	PS
lptB	44	lipopolysaccharide export ABC transporter ATPase	CS
hcaT	45	putative 3-phenylpropionic transporter	ME
fabG	45	3-oxoacyl-[acyl-carrier-protein] reductase	ME
csiR	45	transcriptional repressor of csiD	RR
yjgP	46	lipopolysaccharide export ABC permease	CS
dkgA	47	2,5-diketo-D-gluconate reductase A	ME
acpP	49	acyl carrier protein (ACP)	ME
rluB	49	23S rRNA pseudouridine(2605) synthase	PS
yheV	50	DUF2387 family putative metal-binding protein	NC
gldA	51	glycerol dehydrogenase, NAD+ dependent; 1,2-propanediol:NAD+ oxidoreductase	ME
rfaQ	51	lipopolysaccharide core biosynthesis protein	ME
crr	52	glucose-specific enzyme IIA component of PTS	ME
fimA	53	major type 1 subunit fimbrin (pilin)	CS
rffA	53	TDP-4-oxo-6-deoxy-D-glucose transaminase	ME
tap	54	methyl-accepting protein IV	RR
lamB	55	maltose outer membrane porin (maltoporin)	ME
dusA	56	tRNA-dihydrouridine synthase A	PS
dnaA	58	chromosomal replication initiator protein DnaA, DNA-binding transcriptional dual regulator	CC
yjjP	58	DUF1212 family inner membrane protein	CS
rpoB	58	RNA polymerase, beta subunit	PS
thrS	59	threonyl-tRNA synthetase	ME
yjgR	60	DUF853 family protein with NTPase fold	NC
yheN	60	sulfurtransferase for 2-thiolation step of mnm(5)-s(2)U34-tRNA synthesis	PS
leuE	61	leucine efflux protein	ME
mtgA	62	biosynthetic peptidoglycan transglycosylase	CS
yfeX	63	porphyrinogen oxidase, cytoplasmic	ME
nemA	63	chromate reductase, quinone reductase, FMN-linked; N-Ethylmaleimide reductase; old yellow enzyme	ME
csdE	64	CsdA-binding activator; Fe-S protein	ME
fre	65	NAD(P)H-flavin reductase	ME
yrfG	65	GMP/IMP nucleotidase	ME
ygiC	66	ATP-Grasp family ATPase	ME
sspA	66	stringent starvation protein A, phage P1 late gene activator, RNAP-associated acid-resistance protein, inactive glutathione S-transferase homolog	RR
wbbJ	67	putative lipopolysaccharide biosynthesis O-acetyl transferase	ME
rdgB	68	dITP/XTP pyrophosphatase	CS
yceH	71	UPF0502 family protein	NC
lldR	75	dual role activator/repressor for lldPRD operon	ME
ysaA	75	putative hydrogenase, 4Fe-4S ferredoxin-type component	ME
rpsJ	75	30S ribosomal subunit protein S10	PS
aaeB	76	p-hydroxybenzoic acid efflux system component	CS
ytjA	76	uncharacterized protein	NC
greB	76	transcript cleavage factor	PS
clpP	78	proteolytic subunit of ClpA-ClpP and ClpX-ClpP ATP-dependent serine proteases	ME
gltP	78	glutamate/aspartate:proton symporter	ME
glnE	83	fused deadenylyltransferase/adenylyltransferase for glutamine synthetase	PS
rne	83	endoribonuclease; RNA-binding protein;RNA degradosome binding protein	PS
deaD	83	ATP-dependent RNA helicase	PS
luxS	85	S-ribosylhomocysteine lyase	RR
pstB	91	phosphate ABC transporter ATPase	CS
pepA	95	multifunctional aminopeptidase A: a cyteinylglycinase, transcription regulator and site-specific recombination factor	ME
dut	95	deoxyuridinetriphosphatase	ME

Table 1. Continued

Gene	cleaved ACA [Distance to start in nts]	Protein product	Classification
rpsB	97	30S ribosomal subunit protein S2	PS
rpoS	108	RNA polymerase, sigma S (sigma 38) factor	PS

The distance of the MazF cleavage sites to the AUG start codon, the encoded protein products as well as their respective functional clusters are given. mRNAs whose cleavage was experimentally verified by primer extension analysis are indicated in bold. (ME = metabolism and energy supply, CC = cell cycle, PS = protein synthesis, RR = response regulation, CS = cell structure, NC = not classified).

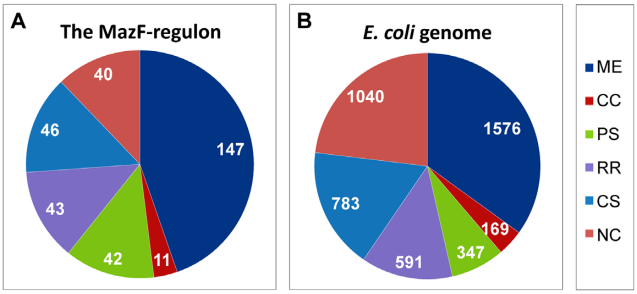

Figure 4. Functional cluster analysis of the MazF-regulon. (**A**) Functional cluster analysis was performed with all 330 MazF-processed and selectively translated mRNAs, comprising the MazF-regulon, according to function assignments provided by *EcoGene 3.0* (27) (**B**) shows the distribution of the functional clusters within the entity of all 4506 *E. coli* genes. (ME = metabolism and energy supply, CC = cell cycle, PS = protein synthesis, RR = response regulation, CS = cell structure, NC = not classified).

protein synthesis is modulated due to selective translation of a subset of processed mRNAs by the concomitantly generated $70S^{\Delta 43}$ ribosomes (5). Recently, several lines of evidence indicate that the activation of TA modules affects persister cell formation. Thus, we aimed to decipher the entity of MazF-processed and selectively translated mRNAs, the 'MazF-regulon', in order to shed light on physiological alterations, which are potentially required for the reprogramming of distinct cells toward persistence. With this end in view, we established a method to isolate intact, full length mRNAs from polysomes, avoiding physiological interference by translation blocking agents and subsequent RNA-sequencing analysis (Figure 1A and Supplementary Table S1). Given the high potential for reciprocal activation of the different TA systems present in *E. coli* as well as their induction by antibiotic treatment, we chose artificial ectopic *mazF* pulse-expression to enrich for immediate MazF targets and to primarily study direct effects of the toxin. Moreover, this approach facilitates the determination of the isolated MazF-mediated effects without induction of additional stress response mechanisms like, e.g. alternative transcription, which would likewise be triggered by physiological stress conditions. As shown in Figure 1, our validation experiments revealed that our approach allows the identification of processed mRNAs entailed by the overexpression of *mazF*. Collectively, this study resulted in the identification of 330 transcripts that are cleaved by MazF within their 5′-UTR and consequently efficiently associated to polysomes upon *mazF* overexpression.

Interestingly, these MazF-processed transcripts are not particularly involved in the stress response, but encode proteins with a broad variety of functions (Figure 4 and Table 1) indicating the widespread effects of MazF activity and consequently translational selectivity in response to stress. In light of the fact that TA systems and in particular the *mazEF* system, are required for persistence (14), we envisage the following model to explain the potential impact of the MazF-mediated stress response on persistence. Our study addresses the entire bacterial population, thus we cannot conclude how transcription and translation are altered in every individual cell. However, given the functional diversity of the proteins encoded by MazF-processed transcripts it is conceivable that MazF induces heterogeneous effects within single cells of the population. Moreover, given the fast reaction to stress conditions triggered solely by degradation of the antitoxin MazE, we hypothesize that the variations introduced by the TA system might differ from cell to cell with regard to their current status, e.g. during different phases of the division cycle or their intrinsic age (31). Thus, MazF could act as a prime effector in response to stress, which might have the potential to amplify the cell variations within a population in an undirected manner and hence would consequently give rise to a variety of heterogeneous cells with distinct physiologies. Moreover, considering the proposed reciprocal activation of different TA systems present in *E. coli* we hypothesize that the interconnected activity of different TA systems further increases the phenotypic variability and in turn stimulates persister cell formation either by induction of stochastic variations in gene expression or by amplification of the molecular noise. This stochastic increase in variability could ensure that a few cells within a population are equipped with a unique toolbox, i.e. a combination of proteins and/or RNAs required to sustain challenging conditions.

The underestimated significance of translational regulation and ribosome specificity

Considering the general stress response, which is mediated primarily at the transcriptional level, one would expect a direct correlation between the transcriptional regulation of a particular mRNA and its translational efficiency as exemplified by its presence in the polysome fraction. However, this assumption is not supported by our first comparative analysis of polysome-associated *versus* total RNA. Interestingly, we observed that the changes in mRNA levels in response to *mazF* overexpression are more pronounced in the polysome-associated mRNA when compared to total RNA (Figure 2A and Supplementary Figure S1C and D). Further, almost 50% of the mRNAs that are differentially associated to polysomes upon *mazF* overexpression are not

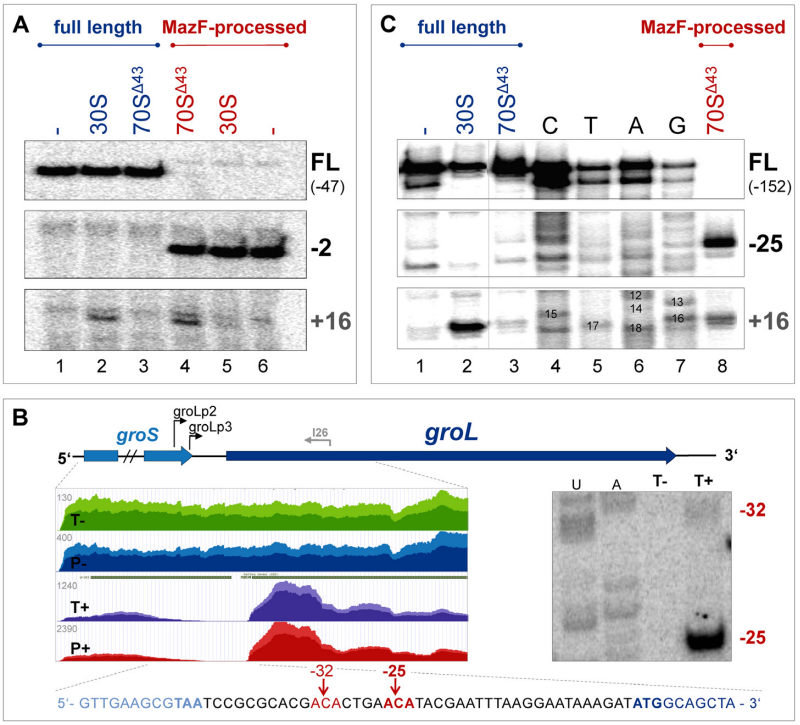

Figure 5. Selective translation initiation of MazF-processed mRNAs by $70S^{\Delta 43}$ ribosomes. (**A**) Toeprinting analysis on full length (blue) and leaderless (red) *rpsU* mRNA using 30S (lanes 2 and 5) and $70S^{\Delta 43}$ ribosomes (lanes 3 and 4). Lanes 1 and 6 ('−'): no ribosomes added. (**B**) Validation of MazF induced cleavage of *groL* by primer extension analysis as described in Figure 3. (**C**) Toeprinting analysis on full length (blue) and leaderless (red) *groL* mRNA using $70S^{\Delta 43}$ ribosomes (lanes 3 and 8). Primer extension analysis on full length *groL* mRNA in the absence of ribosomes (lane 1) and in the presence of 30S ribosomal subunits (lane 2) served as control. The sequencing reaction was performed on full length *groL* mRNA.

significantly regulated at the total RNA level (Supplementary Figure S1A and B). Taken together, our data indicate that in contrast to relaxed conditions, regulation at the level of translation plays a major role in response to stress. This notion was recently strongly supported by Picard *et al*. who analyzed the translational response of the lactic acid bacterium *Lactococcus lactis* during isoleucine starvation by ribosome profiling coupled with microarray analysis (32). The authors present evidence that translational regulation significantly contributes to the stress response. Correspondingly, Taylor *et al*. investigated the extent of translational regulation in protein synthesis of *Shewanella oneidensis MR-1* during oxygen limitation by comparing RNA sequencing and proteome data (32). They report that the alteration of translational efficiency contributes to about 75% of the changes in protein levels.

In our analysis, the entire set of transcripts encoding ribosomal proteins (RPs) intriguingly exemplifies the stress-responsive regulation by selective translation. Here, 46 out of 54 RP-encoding mRNAs are significantly reduced in polysomes after *mazF* overexpression. This is also reflected by the large fraction of 'protein synthesis' transcripts, which are reduced in polysomes after *mazF* overexpression (Supplementary Figure S1C). However, only 14 out of these are also reduced in the total RNA pool. In addition, eleven RP-coding mRNAs (encoding proteins bS1, uS2, uS7, uS10, bS16, bS20, uL2, bL7, uL18, bL28 and bL35 (33)) are processed by MazF and found to be associated with polysomes (Table 1). In contrary, over 50% of all 'cell structure' transcripts are particularly augmented in polysomes after *mazF* overexpression (Supplementary Figure S1C). Together, our observations highlight the significance of translational selectivity, at the level of ribosome heterogeneity and put forward the notion that the immediate response to harsh stress conditions does not rely on the generation of additional regulatory protein or RNA factors.

Selected MazF targets in the spotlight

With respect to their physiological functions associated with the stress response, important candidates for MazF-cleavage are the *rho*, *rpoA*, *zwf* and *rpsA* mRNAs encoding transcription termination factor Rho, the α-subunit of RNAP, the glucose-6-phosphate 1-dehydrogenase and RP bS1, respectively.

The transcription termination factor Rho (Figure 3A) promotes dissociation of the RNA polymerase (RNAP) and the nascent mRNA from the template DNA by ATP-dependent helicase activity upon binding to the so-called *rut* (*r*ho *ut*ilization) sites in the nascent transcript (34,35). It has been shown that transcription and translation are coupled by indirect interaction of the ribosome and RNAP under favorable conditions (36,37). Thereby, frequent *rut* sites within coding regions of mRNAs, that would recruit Rho and hence lead to premature transcription termination, are obscured by the ribosome. When translation is shut down due to stress-induced MazF activity, Rho can access these *rut* sites and promote transcription termination (38). It is conceivable that sustained production of Rho *via* selective

translation of its MazF-processed mRNA might link decreased protein synthesis to early transcription termination in order to save resources for the stressed cells. Furthermore, Rho has been linked to additional regulatory functions in gene expression (38) which might likewise be important during the stress response.

The α-subunit of RNAP (*rpoA*, Figure 3B) is essential for assembly of the core RNAP and involved in the regulation of transcription initiation *via* the α-subunit. Recently, RNAPα was shown to interact with RP uL2 that acts as a transcriptional regulator (39). As we likewise identified the *rplB* transcript coding for uL2 as a MazF target, one could surmise that the transcriptional regulation *via* uL2-RNAPα might be of importance during stress response or stress recovery.

The *zwf* gene (Zwischenferment, Figure 3C) encodes the glucose-6-phosphate 1-dehydrogenase. Interestingly, the penta-peptide NNWDN (Asn-Asn-Trp-Glu-Asn; residues 199–203 of Zwf) is excised from the protein by the ClpPX protease (40) and is likely to be converted to NNWNN (Asn-Asn-Trp-Asn-Asn) by the asparagine synthase A (AsnA) (41). NNWNN represents the quorum sensing molecule '*e*xtracellular *d*eath *f*actor' (EDF), which is secreted into the extracellular environment and thus relays cell density information to the MazEF complex, thereby triggering MazF toxicity (42). Deletion of the genes *zwf* or *asnA* both individually prevented production of active EDF (41). Thus, the removal of the *zwf* 5′-UTR by MazF might ensure the continuous synthesis of the corresponding protein in order to preserve EDF production (43).

Protein bS1 (*rpsA*, Figure 3D) is crucial for efficient translation initiation in Gram-negative bacteria (44–46), but is dispensable for the translation of lmRNAs (47,48). As the MazF-mediated stress response mechanism is based on translation of lmRNAs, bS1 would not be required during stress. However, continuous synthesis of bS1 under these conditions from the leaderless transcript might be crucial to ensure its required presence during recovery from stress when translation of canonical mRNAs becomes prevalent again.

The 'MazF-regulon'

Surprisingly and in contrast to our expectations, the determination of the 'MazF-regulon' revealed that MazF processing of mRNAs does not only result in the formation of lmRNAs. In addition, we identified processing events that leave truncated 5′-UTRs with various lengths. Despite the presence of these 5′-UTRs that comprise the SD sequence these processed transcripts are selectively translated after *mazF* overexpression. Further toeprinting analyses using the leaderless *rpsU* mRNA and the MazF-processed *groL* mRNA that comprises a 25 nts long 5′-UTR verified that $70S^{\Delta 43}$ ribosomes are able to form translation initiation complexes at both MazF-processed transcripts, the leaderless and the leadered mRNA (Figure 5). Taken together, our results indicate that the translational selectivity not only relies on the presence of a 5′-terminal AUG start codon. We hypothesize that MazF-processing by itself primes mRNAs to selective translation by $70S^{\Delta 43}$ ribosomes, rather than being rendered leaderless. Noteworthy, the cleavage by MazF leaves the mRNAs with a 5′-hydroxyl. Consequently, the processed transcripts are not targeted by RNase E and are thus stabilized (49). However, conceptually related to the selective recognition of the 5′ monophosphate by RNase E, we hypothesize that the 5′-hydroxyl might represent a primary feature stimulating the selective interaction with the $70S^{\Delta 43}$ ribosome in the absence of the SD-aSD interaction. Thus, our results raise the possibility that translation of MazF-processed transcripts initiates with the recognition of the 5′-hydroxyl group by the $70S^{\Delta 43}$ ribosomes that are equipped with the initiator tRNA. Subsequently, the $70S^{\Delta 43}$ ribosomes would scan the mRNA downstream to the AUG start codon. As structures within the 5′-UTR would interfere with the scanning process, the removal of structured regions by MazF processing might also stimulate the translational efficiency of the $70S^{\Delta 43}$ ribosomes. However, the underlying mechanism still remains to be elucidated and is currently under study in our laboratory. Nevertheless, our data suggest that the previously described STM (7) has to be redefined. The STM rather comprises $70S^{\Delta 43}$ stress-ribosomes that translate MazF-processed transcripts, independent of the length of the 5′-UTR.

Taken together, our work provides insights into a fast and energy-saving regulatory mechanism that allows bacteria to reprogram protein synthesis in response to harsh changes in environmental conditions. As mentioned above, for this initial approach we ectopically expressed *mazF* in *E. coli* strain MC4100 that harbors the *relA1* mutation (19), to enrich for direct MazF targets. Considering that activation of TA-systems mainly require the stringent response mediated by RelA, it is important to note that our results represent a comprehensive but artificial overview of the MazF-regulon. However, this knowledge will allow and facilitate the determination of distinct MazF-regulons under various physiological stress conditions using the 'wild type' *E. coli* strain MG1655, which is currently ongoing in our group.

SUPPLEMENTARY DATA

Supplementary Data are available at NAR Online.

FUNDING

Austrian Science Fund (FWF) [P22249]; Special Research Program RNA-REG F43 [subproject F4316]; doctoral program RNA-Biology [W1207 to I.M.]. Funding for open access charge: Special Research Program RNA-REG F43 [subproject F4316].
Conflict of interest statement. None declared.

REFERENCES

1. Potrykus,K. and Cashel,M. (2008) (p)ppGpp: still magical? *Annu. Rev. Microbiol.*, **62**, 35–51.
2. Sharma,U.K. and Chatterji,D. (2010) Transcriptional switching in *Escherichia coli* during stress and starvation by modulation of sigma activity. *FEMS Microbiol. Rev.*, **34**, 646–657.
3. Balleza,E., López-Bojorquez,L.N., Martínez-Antonio,A., Resendis-Antonio,O., Lozada-Chávez,I., Balderas-Martínez,Y.I., Encarnación,S. and Collado-Vides,J. (2009) Regulation by transcription factors in bacteria: beyond description. *FEMS Microbiol. Rev.*, **33**, 133–151.

4. Maier,T., Güell,M. and Serrano,L. (2009) Correlation of mRNA and protein in complex biological samples. *FEBS Lett.*, **583**, 3966–3973.
5. Vesper,O., Amitai,S., Belitsky,M., Byrgazov,K., Kaberdina,A.C., Engelberg-Kulka,H. and Moll,I. (2011) Selective translation of leaderless mRNAs by specialized ribosomes generated by MazF in *Escherichia coli*. *Cell*, **147**, 147–157.
6. Zhang,Y., Zhang,J., Hoeflich,K.P., Ikura,M., Qing,G. and Inouye,M. (2003) MazF cleaves cellular mRNAs specifically at ACA to block protein synthesis in *Escherichia coli*. *Mol. Cell*, **12**, 913–923.
7. Moll,I. and Engelberg-Kulka,H. (2012) Selective translation during stress in *Escherichia coli. Trends Biochem. Sci.*, **37**, 493–498.
8. Pandey,D.P. and Gerdes,K. (2005) Toxin-antitoxin loci are highly abundant in free-living but lost from host-associated prokaryotes. *Nucleic Acids Res.*, **33**, 966–976.
9. Wang,X. and Wood,T.K. (2011) Toxin-antitoxin systems influence biofilm and persister cell formation and the general stress response. *Appl. Environ. Microbiol.*, **77**, 5577–5583.
10. Hayes,F. (2003) Toxins-antitoxins: plasmid maintenance, programmed cell death, and cell cycle arrest. *Science*, **301**, 1496–1499.
11. Yamaguchi,Y. and Inouye,M. (2011) Regulation of growth and death in *Escherichia coli* by toxin–antitoxin systems. *Nat. Rev. Microbiol.*, **9**, 779–790.
12. Keren,I., Kaldalu,N., Spoering,A., Wang,Y. and Lewis,K. (2004) Persister cells and tolerance to antimicrobials. *FEMS Microbiol. Lett.*, **230**, 13–18.
13. Lewis,K. (2007) Persister cells, dormancy and infectious disease. *Nat. Rev. Microbiol.*, **5**, 48–56.
14. Tripathi,A., Dewan,P.C., Siddique,S.A. and Varadarajan,R. (2014) MazF-induced growth inhibition and persister generation in *Escherichia coli*. *J. Biol. Chem.*, **289**, 4191–4205.
15. Lewis,K. (2010) Persister cells. *Annu. Rev. Microbiol.*, **64**, 357–372.
16. Ramage,H.R., Connolly,L.E. and Cox,J.S. (2009) Comprehensive functional analysis of mycobacterium tuberculosis toxin-antitoxin systems: implications for pathogenesis, stress responses and evolution. *PLoS Genet.*, **5**, e1000767.
17. Amitai,S., Kolodkin-Gal,I., Hananya-Meltabashi,M., Sacher,A. and Engelberg-Kulka,H. (2009) *Escherichia coli* MazF leads to the simultaneous selective synthesis of both 'death proteins' and 'survival proteins'. *PLoS Genet.*, **5**, e1000390.
18. Ingolia,N.T., Ghaemmaghami,S., Newman,J.R.S. and Weissman,J.S. (2009) Genome-wide analysis *in Vivo* of translation with nucleotide resolution using ribosome profiling. *Science*, **324**, 218–223.
19. Casadaban,M.J. (1976) Transposition and fusion of the lac genes to selected promoters in *Escherichia coli* using bacteriophage lambda and Mu. *J. Mol. Biol.*, **104**, 541–555.
20. Martin,M. (2011) Cutadapt removes adapter sequences from high-throughput sequencing reads. *EMBnet.journal*, **17**, 10–12.
21. Hoffmann,S., Otto,C., Kurtz,S., Sharma,C.M., Khaitovich,P., Vogel,J., Stadler,P.F. and Hackermüller,J. (2009) Fast mapping of short sequences with mismatches, insertions and deletions using index structures. *PLoS Comput. Biol.*, **5**, e1000502.
22. Hoffmann,S., Otto,C., Doose,G., Tanzer,A., Langenberger,D., Christ,S., Kunz,M., Holdt,L.M., Teupser,D., Hackermüller,J. *et al.* (2014) A multi-split mapping algorithm for circular RNA, splicing, trans-splicing and fusion detection. *Genome Biol.*, **15**, R34.
23. Anders,S., Pyl,P.T. and Huber,W. (2014) HTSeq—a Python framework to work with high-throughput sequencing data. *Bioinformatics*, **31**, 166–169.
24. Anders,S. and Huber,W. (2010) Differential expression analysis for sequence count data. *Genome Biol.*, **11**, R106.
25. Kent,W.J., Sugnet,C.W., Furey,T.S., Roskin,K.M., Pringle,T.H., Zahler,A.M. and Haussler,D. (2002) The human genome browser at UCSC. *Genome Res.*, **12**, 996–1006.
26. Wolfinger,M.T., Fallmann,J., Eggenhofer,F. and Amman,F. (2015) ViennaNGS: A toolbox for building efficient next- generation sequencing analysis pipelines. *F1000Research*, **4**, 50.
27. Zhou,J. and Rudd,K.E. (2013) EcoGene 3.0. *Nucleic Acids Res.*, **41**, D613–D624.
28. R Development Core Team (2008) R: a language and environment for statistical computing. *R foundation for statistical computing*. Vienna.
29. Miller,O.L. Jr, Hamkalo,B.A. and Thomas,C.A. Jr (1970) Visualization of bacterial genes in action. *Science*, **169**, 392–395.
30. Wagner,A.F., Schultz,S., Bomke,J., Pils,T., Lehmann,W.D. and Knappe,J. (2001) YfiD of *Escherichia coli* and Y06I of bacteriophage T4 as autonomous glycyl radical cofactors reconstituting the catalytic center of oxygen-fragmented pyruvate formate-lyase. *Biochem. Biophys. Res. Commun.*, **285**, 456–462.
31. Nyström,T. (2007) A bacterial kind of aging. *PLoS Genet.*, **3**, e224.
32. Picard,F., Loubière,P., Girbal,L. and Cocaign-Bousquet,M. (2013) The significance of translation regulation in the stress response. *BMC Genomics*, **14**, 588.
33. Ban,N., Beckmann,R., Cate,J.H., Dinman,J.D., Dragon,F., Ellis,S.R., Lafontaine,D.L., Lindahl,L., Liljas,A., Lipton,J.M. *et al.* (2014) A new system for naming ribosomal proteins. *Curr. Opin. Struct. Biol.*, **24**, 165–169.
34. Peters,J.M., Vangeloff,A.D. and Landick,R. (2011) Bacterial transcription terminators: the RNA 3′-end chronicles. *J. Mol. Biol.*, **412**, 793–813.
35. Boudvillain,M., Nollmann,M. and Margeat,E. (2010) Keeping up to speed with the transcription termination factor Rho motor. *Transcription*, **1**, 70–75.
36. Burmann,B.M., Schweimer,K., Luo,X., Wahl,M.C., Stitt,B.L., Gottesman,M.E. and Rösch,P. (2010) A NusE:NusG complex links transcription and translation. *Science*, **328**, 501–504.
37. Proshkin,S., Rahmouni,A.R., Mironov,A. and Nudler,E. (2010) Cooperation between translating ribosomes and RNA polymerase in transcription elongation. *Science*, **328**, 504–508.
38. Boudvillain,M., Figueroa-Bossi,N. and Bossi,L. (2013) Terminator still moving forward: expanding roles for Rho factor. *Curr. Opin. Microbiol.*, **16**, 118–124.
39. Rippa,V., Cirulli,C., Di Palo,B., Doti,N., Amoresano,A. and Duilio,A. (2010) The ribosomal protein L2 interacts with the RNA polymerase alpha subunit and acts as a transcription modulator in *Escherichia coli*. *J. Bacteriol.*, **192**, 1882–1889.
40. Kolodkin-Gal,I. and Engelberg-Kulka,H. (2008) The extracellular death factor: physiological and genetic factors influencing its production and response in *Escherichia coli*. *J. Bacteriol.*, **190**, 3169–3175.
41. Kolodkin-Gal,I., Hazan,R., Gaathon,A., Carmeli,S. and Engelberg-Kulka,H. (2007) A linear pentapeptide is a quorum-sensing factor required for mazEF-mediated cell death in *Escherichia coli*. *Science*, **318**, 652–655.
42. Belitsky,M., Avshalom,H., Erental,A., Yelin,I., Kumar,S., London,N., Sperber,M., Schueler-Furman,O. and Engelberg-Kulka,H. (2011) The *Escherichia coli* extracellular death factor EDF induces the endoribonucleolytic activities of the toxins MazF and ChpBK. *Mol. Cell*, **41**, 625–635.
43. Kumar,S., Kolodkin-Gal,I., Vesper,O., Alam,N., Schueler-Furman,O., Moll,I. and Engelberg-Kulka,H. (2010) Escherichia coli Quorum-Sensing EDF, A Peptide Generated by Novel Multiple Distinct Mechanisms and Regulated by trans-Translation. *MBio*, **7**, doi:10.1128/mBio.02034-15.
44. Boni,I.V., Isaeva,D.M., Musychenko,M.L. and Tzareva,N.V. (1991) Ribosome-messenger recognition: mRNA target sites for ribosomal protein S1. *Nucleic Acids Res.*, **19**, 155–162.
45. de Smit,M.H. and van Duin,J. (1994) Translational initiation on structured messengers. Another role for the Shine-Dalgarno interaction. *J. Mol. Biol.*, **235**, 173–184.
46. Qu,X., Lancaster,L., Noller,H.F., Bustamante,C. and Tinoco,I. (2012) Ribosomal protein S1 unwinds double-stranded RNA in multiple steps. *Proc. Natl. Acad. Sci. U.S.A.*, **109**, 14458–14463.
47. Moll,I., Grill,S., Gründling,A. and Bläsi,U. (2002) Effects of ribosomal proteins S1, S2 and the DeaD/CsdA DEAD-box helicase on translation of leaderless and canonical mRNAs in *Escherichia coli*. *Mol. Microbiol.*, **44**, 1387–1396.
48. Tedin,K., Resch,A. and Bläsi,U. (1997) Requirements for ribosomal protein S1 for translation initiation of mRNAs with and without a 5′ leader sequence. *Mol. Microbiol.*, **25**, 189–199.
49. Celesnik,H., Deana,A. and Belasco,J.G. (2007) Initiation of RNA decay in *Escherichia coli* by 5′ pyrophosphate removal. *Mol. Cell*, **27**, 79–90.